

Dissociative Photoionization and Thermochemistry of Dihalomethane Compounds Studied by Threshold Photoelectron Photoion Coincidence Spectroscopy

A. F. Lago,[†] James P. Kercher,[†] András Bödi,[‡] Bálint Sztáray,[‡] B. Miller,[†]
D. Wurzelmann,[†] and Tomas Baer^{*,†}

Department of Chemistry, University of North Carolina, Chapel Hill, North Carolina 27599-3290, and
Department of General and Inorganic Chemistry, Eötvös Loránd University, Budapest, Hungary

Received: October 12, 2004; In Final Form: December 2, 2004

The dissociative photoionization studies have been performed for a set of dihalomethane CH_2XY (X, Y = Cl, Br, and I) molecules employing the threshold photoelectron photoion coincidence (TPEPICO) technique. Accurate dissociation onsets for the first and second dissociation limits have been recorded in the 10–13 eV energy range, and ionization potentials have been measured for these compounds. By using our experimental dissociation onsets and the known heat of formation of CH_2Cl_2 molecule, it has been possible to derive the 0 and 298 K heats of formation of all six neutral dihalomethanes as well as their ionic fragments, CH_2Cl^+ , CH_2Br^+ , and CH_2I^+ , to a precision better than 3 kJ/mol. These new measurements serve to fill the lack of reliable experimental thermochemical information on these molecules, correct the old literature values by up to 19 kJ/mol, and reduce their uncertainties. From our thermochemical results it has also been possible to derive a consistent set of bond dissociation energies for the dihalomethanes.

1. Introduction

The interest in the study of the photoionization and thermochemistry of polyhalomethane molecules has increased considerably in the last years. Molecules such as CH_2Br_2 , CH_2I_2 , CH_2BrI , CH_2ICl , and others have been observed in the troposphere, and consequently have been considered important sources of reactive halogens in the atmosphere.^{1–5} From a fundamental viewpoint, dissociative photoionization studies involving polyhalomethane molecules have also attracted recent experimental and theoretical interest as a result of the different dissociation channels that can be identified upon absorption of VUV photons.^{6–10}

Photoionization experiments involving the detection of energy-selected ions in coincidence with initially zero energy electrons are very useful for studying ion dissociation dynamics as well as for the determination of accurate ion thermochemistry.^{11–14} The aim of this work is to investigate the gas-phase dissociative photoionization and thermochemistry of the dihalomethane compounds, namely, CH_2Cl_2 , CH_2I_2 , CH_2Br_2 , CH_2ICl , CH_2IBr , and CH_2BrCl , by the use of threshold photoelectron photoion coincidence (TPEPICO) spectroscopy. The experimental breakdown diagrams, analyzed with the RRKM statistical theory and ab initio calculations, permit the accurate determinations of dissociation onsets, heats of formation, and bond dissociation energies for those molecules and their respective ionic fragments. Threshold photoelectron spectra (TPES) have also been recorded in order to obtain accurate ionization energies for some of these molecules.

Our TPEPICO experiment provides onset energies with errors on the order of ± 10 meV (~ 1 kJ/mol) for the first dissociation limit. Although pulsed field ionization PEPICO experiments¹⁵ and MATI studies^{16,17} are at least an order of magnitude more

accurate, none have been reported for this series of molecules. Furthermore, even if they had been, the derived heats of formation would still be limited by the ancillary heats of formation, such as the ± 1.3 kJ/mol uncertainty in the CH_2Cl_2 heat of formation.

A major advance in the data analysis has permitted us to model accurately the second dissociation limit, which is in competition with the lower energy channel. To determine this onset, it is necessary to model the dissociation rates with the statistical theory of unimolecular decay.^{18–20} The accuracies of these second dissociation limits are within ± 30 meV, which were determined by the data analysis and not by the resolution of the TPEPICO experiment.

With the exception of the CH_2Cl_2 molecule, for which experimental heat of formation has been determined^{21,22} and supported by high-level theoretical calculations,²³ only a few reliable experimental values for heats of formation of the dihalomethane molecules can be found in the literature. Most of the values of neutral and ion heats of formation for those molecules available in the widely used thermochemical tables^{21,24–26} are either estimated values or have error bars as high as 25 kJ/mol. Our results provide the first accurate and self-consistent experimental determination of molecular dissociation onsets, leading to reliable values of 0 and 298 K heats of formation and bond dissociation energies for this set of molecules.

2. Experimental Approach

The aspects of the threshold photoelectron photoion coincidence (TPEPICO) apparatus have been described in detail elsewhere.^{27–29} Briefly, room temperature samples were introduced into the ionization region by means of a capillary and ionized with VUV photons from a hydrogen (H_2) discharge lamp dispersed by a 1 m normal incidence monochromator. The entrance and exit slits were set to 100 μm , which provided a

* Address correspondence to this author. E-mail: baer@unc.edu.

[†] University of North Carolina.

[‡] Eötvös Loránd University.

resolution of 1 Å (~12 meV at a photon energy of 10 eV). The energy scale was calibrated by using the hydrogen Lyman- α resonance line. Ions and electrons were accelerated in opposite directions with the use of a 20 V/cm extraction field. The use of velocity focusing optics³⁰ for electrons yielded an improved resolution of approximately 10 meV.²⁸ Electrons are extracted toward an electrode with a gridless 12.7 mm aperture located 6 mm from the center of the ionization region. A second gridless acceleration electrode 12 mm from the first one accelerates the electrons to 67 eV. Electrons drift approximately 13 cm through a field free flight tube, terminated by an aperture containing a central hole (1.5 mm) and a ring shaped opening with 6 and 10 mm inner and out diameters, respectively. The electrons are then detected by either a Burle channeltron (located on the axis) or a Burle multichannel plate (ring around the axis). Threshold electrons and energetic (hot) electrons along the extraction axis are detected by the channeltron, whereas the energetic electrons with a few meV perpendicular to the extraction axis are collected by the MCP detector. By adopting a hot electron subtraction procedure described previously,³¹ we obtain the hot electron free threshold photoelectron photoion coincidence spectrum (TPEPICO) as well as a threshold photoelectron spectrum (TPES). The ions produced are accelerated over a 5 cm region before drifting 40 cm through the first field free region to a single stage 40 cm long reflectron, where the ions are decelerated and reflected and then drifted through another 40 cm second drift region before being detected on tandem Burle MCPs. The electron and ion signals are used as start and stop pulses for obtaining the ion TOF spectrum. A complete TOF spectrum can be recorded in 1–12 h depending on the signal intensity and the desired signal-to-noise ratio. The collection efficiency was about 32% for threshold electrons and 9% for ions. The samples were purchased from Sigma-Aldrich with purity better than 98% and were used without further purification, except for the CH₂I₂ sample, in which we performed a vacuum distillation prior to use in order to eliminate a small contamination of CH₂I₂ from our CH₂I₂ sample. The purification by distillation was difficult to achieve at atmospheric pressure because the CH₂BrI sample disproportionated to CH₂I₂ and CH₂Br₂ at high temperatures.

3. Theoretical Calculations

The ab initio calculations were carried out using the Gaussian 98 package.³² The ground state geometries of the neutral and ionic species were fully optimized by using density functional theory (DFT), with the Becke 3 parameter and the Lee, Yang, Parr (B3LYP) functional,^{33,34} and the 6-311G* basis set. The vibrational frequencies, required for the RRKM analysis of the experimental breakdown curves, were also obtained in these calculations and are listed, without scaling, in Table 1. To check the validity of using the calculated frequencies without scaling, we tested the simulations with our data using the experimental vibrational frequencies for the CH₂Cl₂ from the literature.³⁵ No difference was noted between the simulations with the calculated and experimental vibrational frequencies. The transition state (TS) vibrational frequencies, required in the fitting of the second dissociation onsets for the mixed dihalomethanes, CH₂BrI, CH₂BrCl, and CH₂ICl, were obtained by stretching the carbon–halogen bonds to approximately 4 Å and calculating the vibrational frequencies at the DFT (B3LYP/6-311G*) level of theory. These frequencies are also shown in Table 1.

4. Results

4.1. Ionization Potentials. Ionization potentials were obtained from our TPEPICO and TPES experiments for all six dihalomethanes.

TABLE 1: Calculated Neutral and Ionic Vibrational Frequencies at the B3LYP/6-311G* Level

species	vibrational frequencies									
CH ₂ Cl ₂	284	697	714	910	1201	1323	1473	3129	3208	
CH ₂ Cl ₂ ⁺	316	540	682	803	1071	1174	1224	2850	2896	
CH ₂ Br ₂	168	568	612	820	1132	1239	1451	3141	3228	
CH ₂ Br ₂ ⁺	162	527	619	883	1053	1202	1438	3141	3257	
CH ₂ I ₂	116	482	572	732	1075	1165	1427	3144	3234	
CH ₂ I ₂ ⁺	113	500	540	789	1011	1127	1411	3142	3257	
CH ₂ BrCl	225	589	709	859	1172	1279	1464	3136	3220	
CH ₂ BrCl ⁺	243	516	520	779	1073	1150	1292	2955	2963	
CH ₂ Cl ⁺ ...Br ^a	−91	177	391	730	1033	1094	1459	3003	3090	
CH ₂ Br ⁺ ...Cl ^a	−80	159	344	535	912	1047	1419	3007	3099	
CH ₂ ICl	192	517	704	801	1158	1242	1457	3139	3223	
CH ₂ ICl ⁺	159	289	638	794	1109	1174	1402	3064	3126	
CH ₂ Cl ⁺ ...I ^a	−101	155	330	762	1026	1066	1455	3100	3187	
CH ₂ I ⁺ ...Cl ^a	−108	117	266	345	742	891	1355	3108	3210	
CH ₂ BrI	141	514	600	770	1111	1205	1441	3143	3230	
CH ₂ BrI ⁺	130	506	594	831	1043	1172	1430	3142	3256	
CH ₂ Br ⁺ ...I ^a	−85	147	238	512	882	970	1382	3163	3271	
CH ₂ I ⁺ ...Br ^a	−66	104	135	398	786	889	1353	3164	3275	

^a Transition state vibrational frequencies.

TABLE 2: Ionization Potentials (eV)

species	IP (this work)	IP (literature)
CH ₂ Cl ₂	11.326 ± 0.006	11.32 ± 0.01 ^a
CH ₂ Br ₂	10.545 ± 0.010	10.52 ± 0.05 ^b
CH ₂ BrCl	10.765 ± 0.010	10.77 ± 0.01 ^c
CH ₂ BrI	9.692 ± 0.012	
CH ₂ I ₂	9.420 ± 0.030	10.46 ± 0.02 ^b
CH ₂ ICl	9.752 ± 0.012	

^a Werner et al.³⁶ ^b Tsai et al.³⁷ ^c Novak et al.³⁸

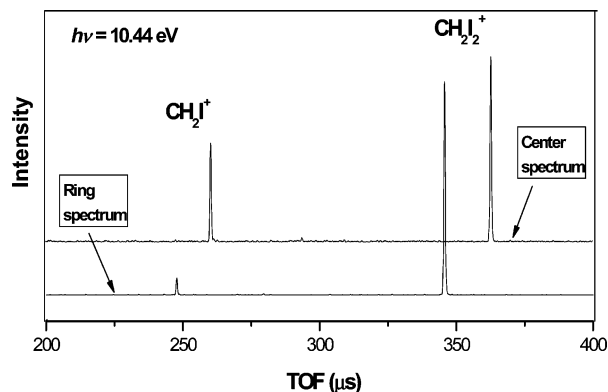


Figure 1. TOF distributions for parent ion and CH₂I⁺ fragment from CH₂I₂ for the center (above) and ring (below) PEPICO spectra. The differences in the time-of-flight for the peaks in the center and ring spectra are solely for presentational purposes.

ethanes. The results are presented in Table 2, which also shows the most reliable experimental values available from the literature.^{36–38} From Table 2 we observe that, in general, our results are in good agreement with the literature values. In addition, in this work we also present the first experimental values of ionization potential for the mixed dihalomethanes CH₂BrI and CH₂ICl (9.692 ± 0.012 and 9.752 ± 0.012, respectively). The larger error attributed to the IP of CH₂I₂ is a result of the generally broad first band observed in the PES.

4.2. TOF Distribution and Breakdown Diagrams. Typical TOF distributions for the center and ring electrodes for the case of CH₂I₂ are shown in Figure 1. The narrow and symmetric peak shapes in the TOF distributions indicate that the dissociation process is rapid, which means that the rate constant is faster than about 10⁷ s^{−1} so that it cannot be measured. If the rates were slower than that, the TOF distributions would be asym-

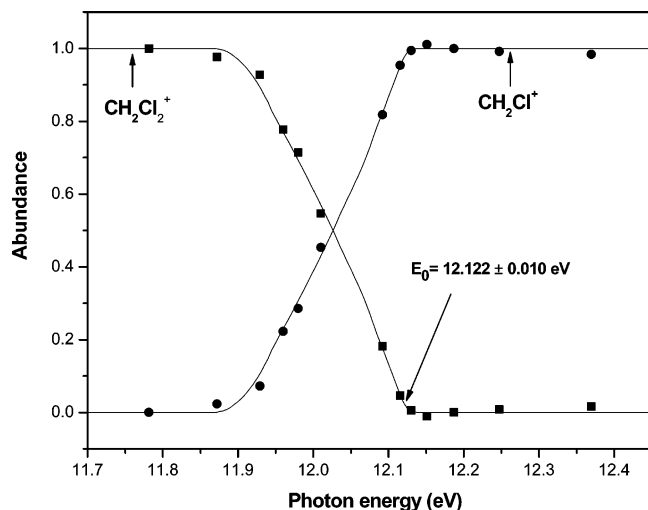


Figure 2. Breakdown diagram for CH_2Cl_2 in the 11.5–12.5 eV range. Solid symbols are the experimental fractional abundances of parent and daughter ions. Solid lines represent the best calculated fit to the experimental data.

metric. The photon energy of 10.44 eV is close to the dissociation limit to $\text{CH}_2\text{I}^+ + \text{I}^*$, so that both parent and fragment ions are observed in the center and ring spectra. The ring spectrum, in which the ions are collected in coincidence with hot electrons, is associated with lower energy ions and thus shows fewer fragment ions than the corresponding center spectrum, in which the ions are detected in coincidence with mostly threshold electrons. By multiplying the ring spectrum by a factor and subtracting it from the center spectrum, we obtain a TPEPICO spectrum that is free of hot electrons. The factor ($f = 0.165$) by which we multiply the ring spectrum is independent of the photon energy and of the molecule. Indeed, it remains constant for several months. It can vary if the collection efficiency of the ring multichannel plate detector or the center channeltron changes. If these collection efficiencies were the same, the factor would be close to the ratio of the geometric areas of the center and ring holes. In practice, the factor of 0.165 is determined experimentally from the TPEPICO spectra at higher energies, as outlined below.

Ion TOF distributions were collected at a number of photon energies from which we obtained the fractional abundance of parent and fragment ions. The integrated peak areas from the center and ring TOF spectra were used in order to generate the corrected breakdown diagrams, $B(I)$, by eq I:³¹

$$B(I) = \frac{(I_c) - f(I_r)}{(T_c) - f(T_r)} \quad (\text{I})$$

where I_c and T_c are the integrated peak areas of an ion and the total area of the parent and daughter ions associated with the center electrode, respectively. The same holds for I_r and T_r with respect to the ring electrode. The experimental subtraction factor f (0.165) was obtained from the ratio of the center and ring TOF peak areas for the parent ion at energies well above the dissociation limit. At these energies, no parent ions should be observed because the dissociation is rapid. Thus all observed parent ions must be associated with hot electron coincidences.

The breakdown diagrams obtained for the six dihalomethane molecules in the range from 10 to 13 eV are shown in Figures 2–7. The rapid dissociation of these ions is not only evident from the symmetric TOF distributions for the daughter ions, but it is also confirmed by the excellent fit of our calculated

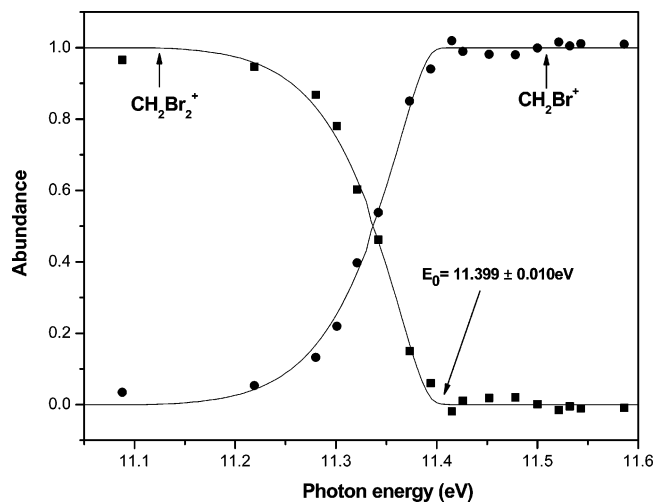


Figure 3. Breakdown diagram for CH_2Br_2 in the 11–11.6 eV range.

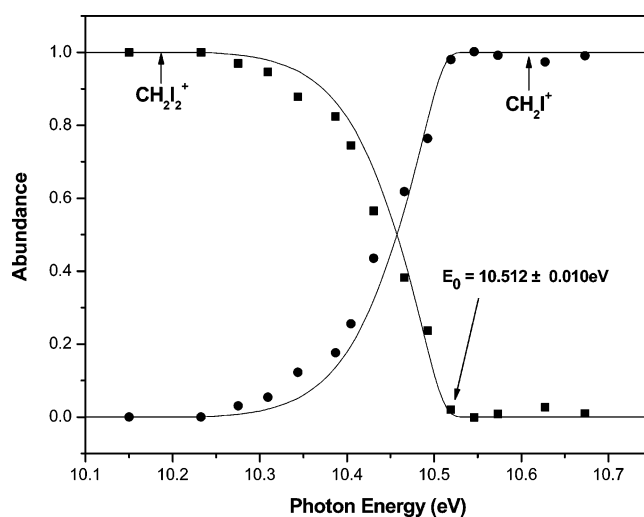


Figure 4. Breakdown diagram for CH_2I_2 in the 10.1–10.7 eV range.

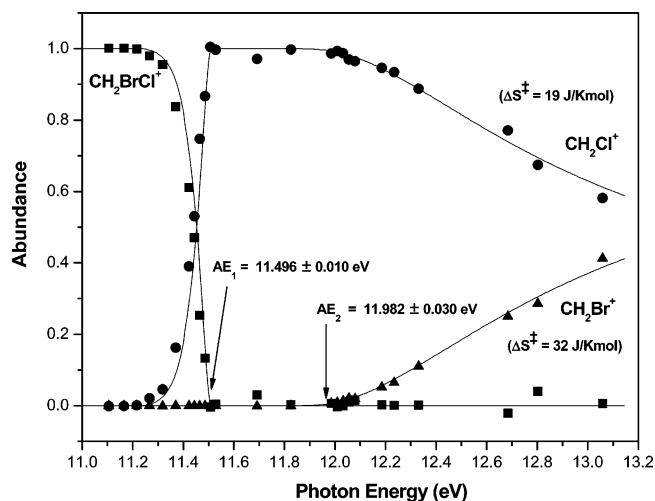


Figure 5. Breakdown diagram for CH_2BrCl in the 11–13.2 eV range.

and measured breakdown diagram for the first dissociation channel. The solid lines represent the calculated breakdown curves in which the internal energy distribution of the molecules, $P(E)$, defined as the number of states per unit energy,²⁰ is taken into account, and which assumes that all ions with internal energies in excess of the dissociation limit will fragment.

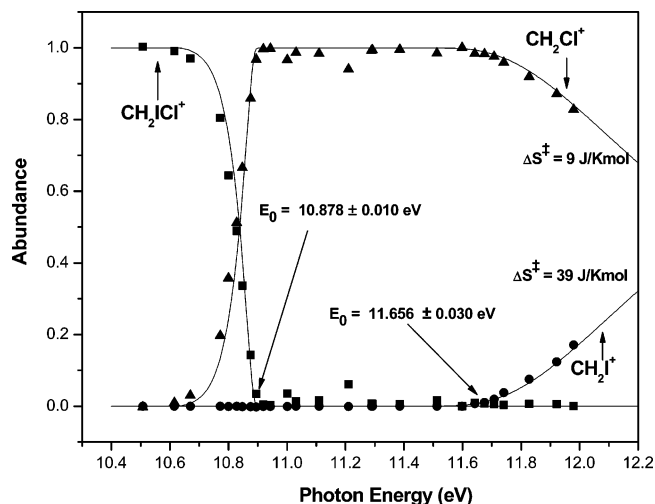


Figure 6. Breakdown diagram for CH_2ICl in the 10.4–12.2 eV range.

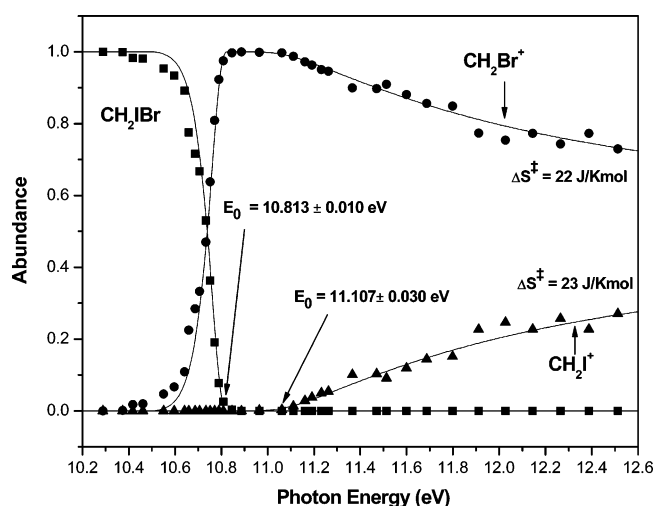


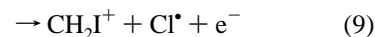
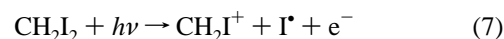
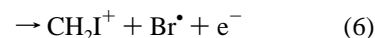
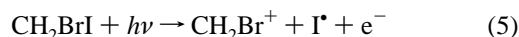
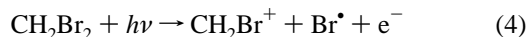
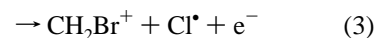
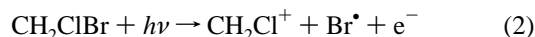
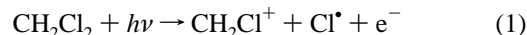
Figure 7. Breakdown diagram for CH_2IBr in the 10.2–12.6 eV range.

In the fitting of the first dissociation onset for these six dihalomethane molecules, the only adjustable parameter is the 0 K dissociation limit (E_0), in which the approach of the curve to the first dissociation limit (E_{01}) is determined by the neutral thermal energy distribution, as previously described by Fogleman et al.²⁹ This energy distribution is calculated with vibrational frequencies and rotational constants obtained from the B3LYP/6-311G* level. As already mentioned, the results for the CH_2Cl_2 analysis, where experimental vibrational frequencies are available, were identical with those of the simulation using the unscaled calculated frequencies.

For the case of the mixed dihalides, a second dissociation onset at somewhat higher photon energies is observed in competition with the first fragmentation channel. As evident in Figures 5–7, the second onset (E_{02}) is much less sharp. The reason is that the rate constant for the second halogen atom loss at its onset is $1/h\rho(E_{02})$, whereas the rate constant at that energy for the first halogen atom loss is $N^\ddagger(E_{02} - E_{01})/h\rho(E_{02})$, a rate that can be orders of magnitude higher than the previous one. This can shift the appearance energy for the second fragment to a higher energy by the competitive shift^{39–41} and it prevents the observation of a step in the fragment ion signal at its dissociation limit. To fit the slow fall in the first fragment ion signal and the slow rise of the second fragment ion signal, it is necessary to calculate the relative rate constants of the two dissociation reactions, which requires knowledge of the molecular ion and the transition state frequencies of the two

reaction channels. These were obtained as explained in section 3. Because the rate constants are larger than experimentally measurable by our TPEPICO experiment, only the relative rate constants are important. We thus determined the transition state parameters for the first reaction by extending the C–X bond to approximately 4 Å and calculating the vibrational frequencies, which are listed in Table 1. At this geometry, the reaction coordinate (C–X stretch) frequency is imaginary (negative) and the two C–X bending modes, which ultimately turn into rotations, have considerably lower vibrational frequencies. The rest of the vibrational frequencies remain relatively unaffected (see Table 1). We repeat this procedure by calculating the vibrational frequencies for the ion with the C–Y bond extended to approximately 4 Å. The two reduced bending frequencies are then adjusted until the second onset in the breakdown diagram is fitted. It is evident that the second onset, E_{02} , affects primarily the point where the signal first appears, whereas the TS frequencies for the second onset determine the calculated slope of the line. Thus, the two parameters are somewhat uncoupled. Nevertheless, the resulting error associated with this two-parameter fitting of the breakdown diagram is generally higher (about ± 30 meV).

4.3. Dissociation Onsets and Thermochemistry. The present work is concerned with the determination of the 0 K dissociation onsets and thermochemistry of the dihalomethane neutral molecules and fragment ions following reactions 1–9:



Our measured dissociation onsets are presented in Figures 2–7 and summarized in the form of a diagram in Figure 8. The energy reference, set to 0, for this figure is $\text{CH}_2\text{Cl}_2 + 2\text{Br} + 2\text{I}$. The atoms are not shown in this figure for clarity of presentation. Thus, according to our measurement, the relative energy of $\text{CH}_2\text{ICl} + \text{Cl} + 2\text{Br} + \text{I}$ is 1.244 eV. The onset energies listed in Figure 8 are considerably more accurate than the previously published values. In addition, there is a built in degeneracy in our data set. For instance, we can determine the energy of $\text{CH}_2\text{BrI} + 2\text{Cl} + \text{Br} + \text{I}$ by going to the left or to the right. If our measurements were perfect, we would be able to obtain the same value for the CH_2BrI energy going in either direction. That is, we have 8 unknowns and 9 onset measurements. The first attempt provided values for the energy of CH_2BrI that agreed within about 30 meV, which is the result of accumulated error in the measurements, estimated (as upper limits) to be about 10 meV for the first onset determinations and 30 meV for the second ones. By slightly adjusting the three second onsets it was possible to make the difference for the

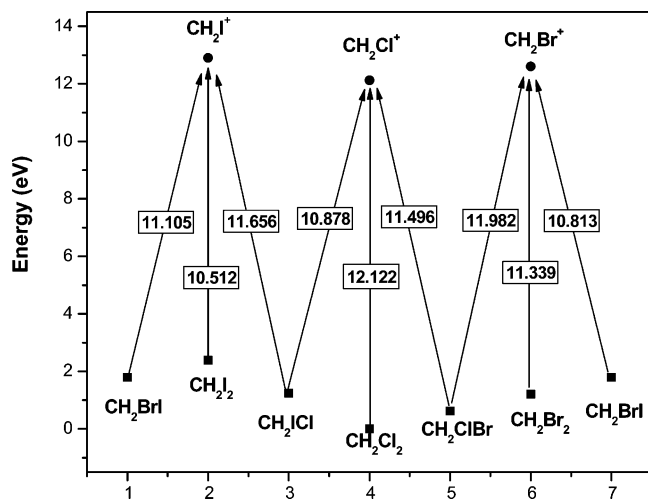


Figure 8. Dissociation onset diagram for the dihalomethane molecules. The energy origin is referenced to $\text{CH}_2\text{Cl}_2 + 2\text{Br} + 2\text{I}$, although for the sake of clarity, the atoms are not included in the figure.

CH_2BrI energies in the cycle vanish without compromising the fitting of the experimental data. As the total error was only 30 meV, the adjustment per each second onset was only about 10 meV, which is well within the upper error limits of ± 30 meV. The solid lines in Figures 2–7 were obtained with these adjusted onsets.

The derived onsets shown in Figure 8 can be compared to other onsets reported in the literature. Photoionization studies for the CH_2Cl_2 molecule reported by Werner et al.³⁶ attempted to take into account the thermal energy. The published dissociation onset value of 12.14 ± 0.020 eV agrees with the present results within the error margin. Holmes et al.⁴² reported a value of 12.10 eV for this onset from their monoenergetic electron ionization experiments, but no error bar was given. Chiang et al.⁶ recently studied the dissociative photoionization of CH_2Cl_2 using synchrotron radiation, and reported a value of 12.08 ± 0.02 eV for the appearance energy of the CH_2Cl^+ ion. This result is about 40 meV below our value, which we attribute to the neglect of the thermal energy contribution to the dissociation onset. Tsai et al.³⁷ reported the CH_2Br^+ from $\text{CH}_2\text{-Br}_2$ and CH_2I^+ from CH_2I_2 onsets recorded by a TPEPICO apparatus. However, they did not correct for hot electrons. Their onsets of 10.55 ± 0.020 and 11.35 ± 0.020 eV, for CH_2I_2 and CH_2Br_2 , respectively, differ from the present results by more than the error margin. More recently, Ma et al.⁴³ reported a Br loss onset from CH_2Br_2 of 11.27 eV. This lower value is probably a result of the neglect of the thermal energy.

The activation entropies ΔS^\ddagger have also been determined for the mixed dihalomethanes, from the calculated vibrational frequencies, and the results are listed in Figures 5–7. The ΔS^\ddagger for the first dissociation depends on our choice of the TS frequencies and is thus arbitrary. On the other hand, once these frequencies are fixed, we vary the TS frequencies for the higher energy dissociation step until we achieve a fit to our data as shown in Figures 5–7. From these fits we thus obtain the difference in the activation entropies, i.e., $\Delta\Delta S^\ddagger$, between the first and the second dissociation channels. In all cases the ΔS^\ddagger is bigger for the lighter atom loss. This is because we convert a higher frequency vibrational mode into a rotation. As expected, the biggest $\Delta\Delta S^\ddagger$ value is between I and Cl loss.

As summarized in Table 3, all of the dihalomethane molecules have heats of formation listed in the literature. However, the only well-established value is that of CH_2Cl_2 . The experimental

TABLE 3: Summary of the Thermochemical Results (kJ/mol) for the Dihalomethanes

species	$\Delta_f H^\circ_{0\text{K}}$	$\Delta_f H^\circ_{298\text{K}}$	$H^\circ_{298\text{K}} - H^\circ_{0\text{K}}^a$	$\Delta_f H^\circ_{298\text{K}}$
CH_2Cl_2	-88.7	-95.5 ± 1.3	11.87	-94.6 ± 8.3^b -95.7 ± 0.8^c -95.5 ± 1.3^d $(959.0)^{c,l}$
CH_2Cl^+	961.1	957.0 ± 1.7	10.13	949.8 ± 8.3^e 0.0 ± 4^c 5.7 ± 5^e 12.5 ± 8.3^k
CH_2Br_2	24.5	3.2 ± 3.4	12.69	$-44.8 \pm 8.3^{b,m}$ $-45.0 \pm 5^{g,h}$ $(937.0)^{c,l}$ 974.9 ± 8.3^e
CH_2BrCl	-30.0	-44.1 ± 1.9	12.27	57.1 ± 20^b $1020.9 \pm 8.3^{e,f}$ 117.6 ± 8.3^b 118.0 ± 21^c 119.5 ± 2.2^i 13.6 ± 20^b 5 ± 25^j
CH_2Br^+	1006.2	994.7 ± 3.3	10.26	
CH_2BrI	70.4	55.0 ± 3.4	12.98	
CH_2I^+	1023.9	1018.2 ± 4.4	10.40	
CH_2I_2	117.0	107.5 ± 4.5	13.25	
CH_2ClI	18.8	10.7 ± 1.9	12.47	

^a For the $H^\circ_{298\text{K}} - H^\circ_{0\text{K}}$ calculations, the heat capacity of the electron was chosen as 0.0 kJ/mol at all temperatures (Ion Convention²⁵). Values obtained using the vibrational frequencies listed in Table 1. ^b Kudchadker and Kudchadker.²⁴ ^c Lias et al.²⁵ ^d Chase²¹ ^e Papina et al.⁴⁴ ^f Holmes et al.⁴² ^g Skorobogatov et al.⁴⁵ ^h Seetula.⁴⁶ ⁱ Pedley.²⁶ ^j Skorobogatov et al.⁴⁷ ^k Bernstein.⁴⁸ ^l Estimated values (no error margin provided). ^m Lias et al.²⁵ misquoted as +45 kJ/mol the heat of formation value of CH_2BrCl (-44.8 kJ/mol) from Kudchadker and Kudchadker.²⁴

$\Delta_f H^\circ_{298}[\text{CH}_2\text{Cl}_2]$ value of -95.5 ± 1.3 kJ/mol (-88.66 kJ/mol at 0 K) taken from the literature²¹ agrees with the value (-95.1 ± 2.5 kJ/mol) recommended by Manion,²² and is also supported by recent high level calculations performed by Feller et al.,²³ which predicted a value of -93.8 ± 2.0 kJ/mol for the $\Delta_f H^\circ_{298}[\text{CH}_2\text{Cl}_2]$. We thus used the literature value of -95.5 kJ/mol, converted to -88.66 kJ/mol at 0 K, to determine the 0 K heats of formation of all other species. We also used the following literature values²¹ for the $\Delta_f H^\circ_{0\text{K}}[\text{X}^*]$ of the atomic elements: 119.62 kJ/mol for Cl^* , 117.92 kJ/mol for Br^* , and 107.16 kJ/mol for I^* .

The procedure used for determining the heats of formation of the dihalomethanes from the experimental dissociation onsets is explained as follows: By measuring the 0 K dissociation onset energy, E_0 , for reaction 1 it is possible to derive the heat of formation of the CH_2Cl^+ ion, using the well-established literature heat of formation values²¹ for CH_2Cl_2 (-88.66 kJ/mol at 0 K) and Cl^* (119.62 kJ/mol at 0 K) in eq II

$$E_0 = \Delta_f H^\circ_{0\text{K}}(\text{CH}_2\text{X}^+) + \Delta_f H^\circ_{0\text{K}}(\text{X}^*) - \Delta_f H^\circ_{0\text{K}}(\text{CH}_2\text{XY}) \quad (\text{II})$$

where X and Y in eq II are halogen atoms (Cl, Br, or I). Note that the above equation is valid at 0 K, but not at 298 K. The resulting heat of formation of CH_2Cl^+ can be used in reaction 2, with the corresponding dissociation onset, to determine the heat of formation of the CH_2ClBr neutral molecule. The $\text{CH}_2\text{-ClBr}$ heat of formation provides a means for determining the heat of formation of CH_2Br^+ from the onset energy for reaction 3, which leads to a measurement of the CH_2Br_2 heat of formation via reaction 4, and so on. The derived 0 K heats of formation can be converted to 298 K values. Table 3 lists both the derived 0 K and the converted 298 K values, which are compared with literature values at 298 K. The conversion for the heat of

formation from 0 to 298 K and vice versa can be made by means of the usual thermochemical cycle, given by eq III:

$$\Delta_f H_{0\text{K}}^\circ = \Delta_f H_{298\text{K}}^\circ - [H_{298\text{K}}^\circ - H_{0\text{K}}^\circ](\text{molecule/ion}) + [H_{298\text{K}}^\circ - H_{0\text{K}}^\circ](\text{elements}) \quad (\text{III})$$

We used the $H_{298\text{K}}^\circ - H_{0\text{K}}^\circ$ literature values⁴⁹ for the atomic elements, and the calculated vibrational frequencies and $H_{298\text{K}}^\circ - H_{0\text{K}}^\circ$ values for the molecules and fragment ions, as listed in Tables 1 and 3, respectively. Our calculated $H_{298\text{K}}^\circ - H_{0\text{K}}^\circ$ values listed in Table 3 are in very good agreement with the ones available in the literature.²⁴ The resulting $\Delta_f H_{298\text{K}}^\circ$ values obtained via eq III are compared to the 298 K literature values. The error bars for the 0 K heats of formation, omitted from Table 3 for the sake of clarity, are the same as the ones attributed to the corresponding 298 K heats of formation.

Among the neutral dihalomethane molecules, in general, our heats of formation for CH_2BrCl , CH_2Br_2 , and CH_2BrI agree well with the literature values, although the error limits have been greatly reduced. However, in the case of the mixed dihalomethanes and fragment ions striking differences have been observed in the values of heats of formation. For instance, the estimated heat of formation for the CH_2ICl available in the literature varies from 5 kJ/mol to 13.6 kJ/mol and with error bars as high as 25 kJ/mol. No experimental heat of formation has been found in the literature for this molecule. Our 298 K value, 10.7 kJ/mol, agrees within the error margins of the literature values, but again we reduce the uncertainty to about 2 kJ/mol. The most important disagreement is found in the case of the CH_2I_2 molecule, whose literature value should be adjusted downward by approximately 10 kJ/mol. A calculated value of 113 kJ/mol for the CH_2I_2 heats of formation⁵⁰ is closer to our measured 107.5 kJ/mol value, but no error bar was given. Among the ions, the major literature discrepancy found was in the case of $\Delta_f H_{298\text{K}}^\circ[\text{CH}_2\text{Br}^+]$, which should be increased by at least 19 kJ/mol, followed by the heat of formation for the CH_2Cl^+ ion, which should also be adjusted.

These reliable heats of formation provide a new perspective for understanding important atmospheric reactions.^{51,52} For instance, it has been suggested that halogen chemistry via reactions such as $\text{Cl}^\bullet + \text{CH}_2\text{ICl} \rightarrow \text{CH}_2\text{Cl}_2 + \text{I}^\bullet$, may have an important influence on the HO_2/OH as well as NO_2/NO concentration ratios of the troposphere, and consequently on its oxidizing capacity.⁵³ To understand the role played by compounds such as CH_2I_2 , CH_2ICl , and other halomethanes in the atmosphere and the extent of their reactions with relevant atmospheric species, information concerning the thermochemistry, kinetics, and mechanism of those compounds are clearly required. Our present results also provide an important route for obtaining heats of formation of other species, including the free radicals, such as $\text{CH}_2\text{Cl}^\bullet$, $\text{CH}_2\text{Br}^\bullet$, and $\text{CH}_2\text{I}^\bullet$. These values can be obtained from the measured ionization energies of the radicals in combination with our corresponding ion heats of formation. Another possible route of obtaining additional thermochemical data is by combining our dihalomethane heats of formation with measured bond dissociation energies.

Bond dissociation energies (BDE) have been obtained in the present work for the $\text{Y}-\text{CH}_2\text{X}$ species (where X and Y are Cl, Br, or I atoms), from our neutral molecular heats of formation, combined with the corresponding recommended experimental heat of formation values for the neutral halomethyl radicals (121.3 kJ/mol for CH_2Cl , 167.4 kJ/mol for CH_2Br , and 217.6 kJ/mol for CH_2I) taken from the literature,^{54,55} and atomic heats of formation from the NIST-JANAF thermochemical tables.²¹

TABLE 4: Carbon–Halogen Bond Dissociation Energies for the Dihalomethanes, Where Y Represents a Halogen Atom

species	bond dissociation energies (kJ/mol)		
	Cl	Br	I
$\text{Y}-\text{CH}_2\text{Cl}$	338.0 ± 3.3	277.3 ± 3.6	217.4 ± 3.6
$\text{Y}-\text{CH}_2\text{Br}$	332.8 ± 4.6	276.1 ± 5.3	219.2 ± 5.4
$\text{Y}-\text{CH}_2\text{I}$	328.2 ± 6.9	274.5 ± 7.5	216.9 ± 7.9

Our results for all nine bond dissociation energies for these dihalomethanes are listed in Table 4, and were obtained by using eq IV:

$$\text{BDE}(\text{Y}-\text{CH}_2\text{X}) = \Delta_f H(\text{Y}) + \Delta_f H(\text{CH}_2\text{X}) - \Delta_f H(\text{CH}_2\text{XY}) \quad (\text{IV})$$

where X and Y represent halogen atoms. The results presented in Table 4 are consistent and serve to reduce the uncertainties and correct the discrepancies of the literature values for those bond energies, as well as providing the first experimentally based values for the $\text{Br}-\text{CH}_2\text{I}$, $\text{I}-\text{CH}_2\text{Br}$, and $\text{Cl}-\text{CH}_2\text{Br}$ bond dissociation energies. Not many results for the bond dissociation energies of dihalomethanes were found in the general literature,⁵⁶ in part due to the scarcity of accurate values of heat of formation for those molecules, as previously pointed out. The scarcity of experimental and theoretical data is particularly severe for bromine and iodine containing molecules. The accuracy in our bond dissociation energy results, shown in Table 4, has been limited by the uncertainties of the literature values^{54,55} for neutral halomethyl radical heats of formation.

As a first observation, despite the fact that quite often it is assumed that all aromatic C–X bond energies are the same for a given halogen atom X (because of the low accuracy usually associated with those measurements), our results from Table 4 show an interesting pattern, where the BDE values are observed to decrease as one goes down in the series and also that the difference between those values gets smaller as one goes from C–Cl to C–I bonds.

The literature values for the $\text{Cl}-\text{CH}_2\text{Cl}$ bond dissociation energy are in the range from 325.1 to 338.0 kJ/mol. Most of the available BDE values in the literature for those molecules were obtained from estimations. Our result of 338.0 kJ/mol matches exactly with the experimental value listed in the literature,^{55,54} since we have taken the same corresponding heats of formation as the starting point for the determination of our present results. However, in the case of the $\text{Br}-\text{CH}_2\text{Br}$ bond, our BDE value of 276.1 kJ/mol is 14 kJ/mol lower than the available experimental value (290.1 ± 9.9 kJ/mol) from the literature.^{54,55} On the other hand, our result agrees very well with the 275.3 kJ/mol reported by Chen et al.⁵⁷ from their electron attachment experiments and also with the calculated value of 275.4 kJ/mol reported by the Lazarou et al.,⁵⁴ using the B3P86/6-311++G(2df,p) level of theory. The BDE values for $\text{I}-\text{CH}_2\text{I}$ found in the literature present a high level of uncertainty, ranging from 203.3 to 230.0 kJ/mol. Our value of 216.9 kJ/mol is about 10 kJ/mol above the experimental value (206.3 ± 7.9 kJ/mol) reported by DeMore et al.⁵⁵ and about 13 kJ/mol below the value (230.0 ± 1 kJ/mol) estimated by Skorobogatov et al.⁴⁷ Nevertheless, our result agrees with the experimental value of 215.7 kJ/mol reported by Carson et al.⁵⁸ and with the value (217.7 kJ/mol) calculated by Lazarou et al.,⁵⁴ obtained at the B3P86/6-311++G(2df,p) level of theory. Among the mixed dihalomethanes, not much information is found in the literature. The BDE values of 206.6 ± 0.8 kJ/mol for $\text{I}-\text{CH}_2\text{Cl}$ and 253.4 ± 1.8 for $\text{Br}-\text{CH}_2\text{Cl}$ have been estimated by Skorobogatov et al.^{47,45} These values differ from our present

results by approximately 11 and 24 kJ/mol, respectively, reflecting the inaccuracy of the molecular and radical heats of formation used in their estimations. Our results are, on the other hand, in good agreement with the values obtained from theoretical calculations for the Cl–CH₂I (326.4 kJ/mol) and I–CH₂Cl (225.6 kJ/mol) bond energies reported by Kambanis et al.⁵⁹

As a final observation, we point out that the value of 301.2 kJ/mol reported as an upper limit for the Cl–CH₂I bond energy by Arunan et al.,⁶⁰ using the infrared chemiluminescence technique, and used as reference by Luo,⁵⁶ has been confirmed neither by our present result (328.2 kJ/mol) nor by theoretical calculations (326.4 kJ/mol).⁵⁹ It may suggest that the infrared chemiluminescence is not the most adequate technique for deriving reliable bond dissociation energies of dihalomethanes. The interpretation of the infrared chemiluminescence data usually requires accurate thermochemical information, which particularly was not available for the CH₂ICl molecule. Other important sources of error in the C–Cl bond energy reported by Arunan et al.⁶⁰ are related to the activation energy (E_a) for the reaction $H + CH_2ICl \rightarrow HCl + CH_2I$, and thermal energy (T_{th}) for the CH₂ICl molecule, required for the bond energy determination, which have not been measured in their work as well. Their estimated E_a value, which was based only on the comparison of the HCl(*v*) IR emission intensities from reaction $H + CH_2ICl$ with the ones from reaction $H + Cl_2$, and also the estimation for the thermal energy (at 300 K), may explain the discrepancy observed for their estimated Cl–CH₂I bond energy value, as compared to the theoretical value⁵⁹ and to our present result. No experimental or theoretical results have been found in the literature for the Br–CH₂I, I–CH₂Br, and Cl–CH₂Br bond dissociation energies.

5. Summary and Conclusions

Dissociative photoionization and thermochemistry have been investigated for a set of dihalomethanes, CH₂XY, (X, Y, = Cl, Br, and I), by using the threshold photoelectron photoion coincidence (TPEPICO) technique. Accurate ionization energies, breakdown diagrams, and dissociation onsets for the first and second dissociation limits have been obtained for those molecules and their ionic fragments. The accuracy of the derived onsets was confirmed by a redundancy in the measurements, in which nine measurements were used to derive eight unknown neutral and ion energies. By using the known heat of formation of CH₂Cl₂, it has been possible to determine the 0 and 298 K heats of formation of CH₂Br₂, CH₂I₂, CH₂BrCl, CH₂BrI, and CH₂ICl neutrals, as well as CH₂Cl⁺, CH₂Br⁺, and CH₂I⁺ ions, to a precision better than 3 kJ/mol. Our new results provide the first accurate and consistent experimental determination of heats of formation for this set of molecules, which serve to correct the $\Delta_f H^\circ_{298K}$ literature values by as much as 19 kJ/mol. Consequently, we were also able to derive reliable bond dissociation energies for the dihalomethane molecules. Some of these bond energy values have been reported for the first time.

Acknowledgment. The authors thank the U.S. Department of Energy for support this work. A.F.L. wishes to gratefully acknowledge the postdoctoral fellowship from CNPq-Brazil.

References and Notes

- Class, T.; Ballschmiter, K. *J. Atmos. Chem.* **1988**, *6*, 35–46.
- Alicke, B.; Hebestreit, K.; Stutz, J.; Platt, U. *Nature* **1999**, *397* (6720), 572–573.
- Heumann, K. G. *Anal. Chim. Acta* **1993**, *283*, 230–245.
- Mossigner, J. C.; Shallcross, D. E.; Cox, R. A. *J. Chem. Soc., Faraday Trans.* **1998**, *94*, 1391–1396.
- Carpenter, L. J.; Sturges, W. T.; Penkett, S. A.; Liss, P. S.; Alicke, B.; Hebestreit, K.; Platt, U. *J. Geophys. Res.* **1999**, *104*, 1679–1689.
- Chiang, S. Y.; Bahou, M.; Sankaran, K.; Lee, Y. P.; Lu, H. F.; Su, M. D. *J. Chem. Phys.* **2003**, *118*, 62–68.
- Lago, A. F.; Santos, A. C. F.; de Souza, G. G. B. *J. Chem. Phys.* **2004**, *120*, 9547–9555.
- Sharma, P.; Vatsa, R. K.; Maity, D. K.; Kulshreshtha, S. K. *Chem. Phys. Lett.* **2003**, *382*, 637–643.
- Huang, J. H.; Xu, D. D.; Fink, W. H.; Jackson, W. M. *J. Chem. Phys.* **2001**, *115*, 6012–6017.
- Yang, G. H.; Meng, Q. T.; Zhang, X.; Han, K. L. *Int. J. Quantum Chem.* **2004**, *97*, 719–727.
- Dannacher, J.; Rosenstock, H. M.; Buff, R.; Parr, A. C.; Stockbauer, R.; Bombach, R.; Stadelmann, J. P. *Chem. Phys.* **1983**, *75*, 23–35.
- Das, P. R.; Nishimura, T.; Meisels, G. G. *J. Phys. Chem.* **1985**, *89*, 2808–2812.
- Duffy, L. M.; Keister, J. W.; Baer, T. *J. Phys. Chem.* **1995**, *99*, 17862–17871.
- Li, Y.; Sztáray, B.; Baer, T. *J. Am. Chem. Soc.* **2001**, *123*, 9388–9396.
- Jarvis, G. K.; Weitzel, K. M.; Malow, M.; Baer, T.; Song, Y.; Ng, C. Y. *Rev. Sci. Instrum.* **1999**, *70*, 3892–3906.
- Krause, H.; Neusser, H. J. *J. Chem. Phys.* **1993**, *99*, 6278–6286.
- Park, S. T.; Kim, S. K.; Kim, M. S. *J. Chem. Phys.* **2001**, *114*, 5568–5576.
- Rosenstock, H. M.; Wallenstein, M. B.; Wahrhaftig, A. L.; Eyring, H. *Proc. Natl. Acad. Sci.* **1952**, *38*, 667–678.
- Marcus, R. A.; Rice, O. K. *J. Phys. Colloid Chem.* **1951**, *55*, 894–908.
- Baer, T.; Hase, W. L. *Unimolecular Reaction Dynamics: Theory and Experiments*; Oxford University Press: New York, 1996.
- Chase, M. W. *NIST-JANAF Thermochemical Tables*; American Institute of Physics: New York, 1998.
- Manion, J. A. *J. Phys. Chem. Ref. Data* **2002**, *31*, 124–165.
- Feller, D.; Peterson, K. A.; de Jong, W. A.; Dixon, D. A. *J. Chem. Phys.* **2003**, *118*, 3510–3522.
- Kudchadker, S. A.; Kudchadker, A. P. *J. Phys. Chem. Ref. Data* **1978**, *7*, 1285–1307.
- Lias, S. G.; Bartmess, J. E.; Liebman, J. F.; Holmes, J. L.; Levin, R. D.; Mallard, W. G. *Gas-Phase Ion and Neutral Thermochemistry*; *J. Phys. Chem. Ref. Data* Vol. 17, Suppl. 1; NSRDS; U.S. Government Printing Office: Washington, DC, 1988.
- Pedley, J. B. *Thermochemical Data and Structures of Organic Compounds*; Thermodynamics Research Center: College Station, TX, 1994.
- Baer, T.; Booze, J. A.; Weitzel, K. M. *Vacuum ultraviolet photoionization and photodissociation of molecules and clusters*, 1st ed.; World Scientific: Singapore, 1991; Chapter 5, pp 259–298.
- Baer, T.; Li, Y. *Int. J. Mass Spectrom.* **2002**, *219*, 381–389.
- Fogleman, E. A.; Koizumi, H.; Kercher, J. P.; Sztáray, B.; Baer, T. *J. Phys. Chem. A* **2004**, *108*, 5288–5294.
- Chandler, D. W.; Parker, D. H. *Adv. Photochem.* **1999**, *25*, 59–106.
- Sztáray, B.; Baer, T. *Rev. Sci. Instrum.* **2003**, *74*, 3763–3768.
- Frisch, M. J.; Trucks, G. W.; Schlegel, H. B.; Scuseria, G. E.; Robb, M. A.; Cheeseman, J. R.; Zakrzewski, V. G.; Montgomery, J. A.; Stratmann, R. E.; Burant, J. C.; Dapprich, S.; Millam, J. M.; Daniels, A. D.; Kudin, K. N.; Strain, M. C.; Farkas, Ö.; Tomasi, J.; Barone, V.; Cossi, M.; Cammi, R.; Mennucci, B.; Pomelli, C.; Adamo, C.; Clifford, S.; Ochterski, J.; Petersson, G. A.; Ayala, P. Y.; Cui, Q.; Morokuma, K.; Malick, D. K.; Rabuck, A. D.; Raghavachari, K.; Foresman, J. B.; Cioslowski, J.; Ortiz, J. V.; Baboul, A. G.; Stefanov, B. B.; Liu, G.; Liashenko, A.; Piskorz, P.; Komáromi, I.; Gomperts, R.; Martin, R. L.; Fox, D. J.; Keith, T.; Al-Laham, M. A.; Peng, C. Y.; Nanayakkara, A.; Gonzalez, C.; Challacombe, M.; Gill, P. M. W.; Johnson, B. G.; Chen, W.; Wong, M. W.; Andres, J. L.; Head-Gordon, M.; Replogle, E. S.; Pople, J. A. *GAUSSIAN 98*, Revision A.7; Gaussian, Inc.: Pittsburgh, PA, 1998.
- Becke, A. D. *J. Chem. Phys.* **1993**, *98*, 5648–5652.
- Lee, C.; Yang, W.; Parr, R. G. *Phys. Rev.* **1988**, *B37*, 785–789.
- Shimanouchi, T. *Tables of Molecular Vibrational Frequencies*; *Natl. Stand. Ref. Data. Ser. (NBS) No. 39*; U.S. Government Printing Office: Washington, DC, 1972.
- Werner, A. S.; Tsai, B. P.; Baer, T. *J. Chem. Phys.* **1974**, *60*, 3650–3657.

- (37) Tsai, B. P.; Baer, T.; Werner, A. S.; Lin, S. F. *J. Phys. Chem.* **1975**, *79*, 570–574.
- (38) Novak, I.; Cvitas, T.; Klasinc, L.; Gusten, H. *J. Chem. Soc., Faraday Trans. 2* **1981**, *77*, 2049–2058.
- (39) Chupka, W. A. *J. Chem. Phys.* **1959**, *30*, 191–211.
- (40) Lifshitz, C. *Mass Spectrom. Rev.* **1982**, *1*, 309–348.
- (41) Huang, F. S.; Dunbar, R. C. *J. Am. Chem. Soc.* **1990**, *112*, 8167–8169.
- (42) Holmes, J. L.; Lossing, F. P.; McFarlane, R. A. *Int. J. Mass Spectrom. Ion Processes* **1988**, *86*, 209–215.
- (43) Ma, Z. X.; Liao, C. L.; Ng, C. Y.; Ma, N. L.; Li, W. K. *J. Chem. Phys.* **1993**, *99*, 6470–6473.
- (44) Papina, T. S.; Kolesov, V. P.; Golovanova, Y. G. *Russ. J. Phys. Chem. (Engl. Transl.)* **1982**, *56*, 1666–1669.
- (45) Skorobogatov, G. A.; Dymov, B. P.; Nedozrelova, I. V. *Russ. J. Gen. Chem. (Engl. Transl.)* **1996**, *66*, 1777–1785.
- (46) Seetula, J. A. *Phys. Chem. Chem. Phys.* **2003**, *5*, 849–855.
- (47) Skorobogatov, G. A.; Dymov, B. P.; Nedozrelova, I. V. *Russ. J. Gen. Chem. (Engl. Transl.)* **1996**, *66*, 1786–1792.
- (48) Bernstein, H. J. *J. Phys. Chem.* **1965**, *69*, 1550–1564.
- (49) Wagman, D. D.; Evans, W. H. E.; Parker, V. B.; Schum, R. H.; Halow, I.; Mailley, S. M.; Churney, K. L.; Nuttall, R. L. *The NBS Tables of Chemical Thermodynamic Properties*; J. Phys. Chem. Ref. Data Vol. 11, Suppl. 2; NSRDS; U.S. Government Printing Office: Washington, DC, 1982.
- (50) Lide, D. R.; Kheiaian, H. V. *CRC Handbook of Thermophysical and Thermochemical Data*, Bk&Disk ed.; CRC Press: Boca Raton, FL, 1994.
- (51) Bilde, M.; Sehested, J.; Nielsen, O. J.; Wallington, T. J.; Meagher, R. J.; McIntosh, M. E.; Piety, C. A.; Nicovich, J. M.; Wine, P. H. *J. Phys. Chem. A* **1997**, *101*, 8035–8041.
- (52) Seinfeld, J. H.; Pandis, S. N. *Atmospheric Chemistry and Physics*; Wiley-Interscience: New York, 1998.
- (53) Davis, D.; Crawford, J.; Liu, S.; McKeen, S.; Bandy, A.; Thornton, D.; Rowland, F.; Blake, D. *J. Geophys. Res.* **1996**, *101*, 2135–2147.
- (54) Lazarou, Y. G.; Prosser, A. V.; Papadimitriou, V. C.; Papagiannakopoulos, P. *J. Phys. Chem. A* **2001**, *105*, 6729–6742.
- (55) DeMore, W. B.; Sander, S. P.; Golden, D. M.; Hampson, R. F.; Kurylo, M. J.; Howard, C. J.; Ravishankara, A. R.; Kolb, C. E.; Molina, M. J. *Chemical kinetics and photochemistry data for use in stratospheric modelling*; JPL publication 97-4, 1997.
- (56) Luo, Y.-R. *Handbook of Bond Dissociation Energies in Organic Compounds*; CRC Press: Boca Raton, FL, 2003.
- (57) Chen, E. C. M.; Albyn, K.; Dussack, L.; Wentworth, W. E. *J. Phys. Chem.* **1989**, *93*, 6827–6832.
- (58) Carson, A. S.; Laye, P. G.; Pedley, J. B.; Welsby, A. M. *J. Chem. Thermodyn.* **1993**, *25*, 261–269.
- (59) Kambanis, K. G.; Argyris, D. Y.; Lazarou, Y. G.; Papagiannakopoulos, P. *J. Phys. Chem. A* **1999**, *103*, 3210–3215.
- (60) Arunan, E.; Vijayalakshmi, S. P.; Valera, R.; Setser, D. W. *Phys. Chem. Chem. Phys.* **2002**, *4* (1), 51–59.